MIXED-MODE IMPEDANCE AND REFLECTION COEFFICIENT OF TWO-PORT DEVICES

T. Carrasco[1, *], J. Sieiro[1], J. M. Lopez-Villegas[1], N. Vidal[1], R. Gonzalez-Echevarria[2], and E. Roca[2]

[1]Department of Electronics, Faculty of Physics, University of Barcelona, Marti i Franques 1, Barcelona 08028, Spain

[2]Institute of Microelectronics of Seville, CSIC and University of Seville Avda. Americo Vespucio s/n, Isla de la Cartuja, Seville 41092, Spain

Abstract—From the point of view of mixed-mode scattering parameters, S_{mm}, a two-port device can be excited using different driving conditions. Each condition leads to a particular set of input reflection and input impedance coefficient definitions that should be carefully applied depending on the type of excitation and symmetry of the two-port device. Therefore, the aim of this paper is to explain the general analytic procedure for the evaluation of such reflection and impedance coefficients in terms of mixed-mode scattering parameters. Moreover, the driving of a two-port device as a one-port device is explained as a particular case of a two-port mixed-mode excitation using a given set of mixed-mode loads. The theory is applied to the evaluation of the quality factor, Q, of symmetrical and non-symmetrical inductors.

1. INTRODUCTION

Currently, most of the RFICs are designed to work in differential configuration due to noise immunity. In fact, the majority of the receiver chipsets available in today's market, as well as some of the components that conform them, are fully differential [1, 2]. Obviously, it implies that the figures of merit of these devices are better expressed in terms of mixed-mode scattering parameters (S_{mm}), which were first introduced by Bockelman and Eisenstadt [3, 4]. In spite of their widespread use in RFIC design, there is still some misunderstanding about how the differential (common)-mode input impedance Z_d (Z_c)

must be calculated in terms of S_{mm} when a two-port is seen as a one-port device. Thus, it is usually found that the differential reflection coefficient Γ_d of a two-port device is assumed to be S_{dd} [5–8]. Therefore, the differential input impedance is calculated using the following bilineal impedance transformation

$$Z_{dd} = 2Z_0 \frac{1 + S_{dd}}{1 - S_{dd}} \tag{1}$$

where $2Z_0$ is the differential surge impedance. Certainly, Z_{dd} in (1) coincides with the differential term of the mixed-mode Z-parameter matrix of a two-port device; however, as it has been previously mentioned in [9] and [10], a close look to (1) reveals that such expression only matches with Z_d (i.e., $Z_d = Z_{dd}$) for fully symmetrical two-port devices. For non-symmetrical devices and taking into account the definition of S_{dd}, (1) neglects any conversion to a reflected common-mode power wave. Then, special care must be taken when using (1) as an equivalent expression to Z_d. For instance, the evaluation of the quality factor Q using the next definition

$$Q = \frac{\text{Im}\left\{Z_{dd}\right\}}{\text{Re}\left\{Z_{dd}\right\}} \tag{2}$$

should be only applied to symmetrical topologies. For non-symmetrical inductors, e.g., spiral inductors, (2) wrongly estimates Q, due to the fact that the component boundary conditions are wrongly set, thus the common-mode conversion is completely dismissed. A similar misunderstanding can be pointed out when Z_{cc} is directly related to Z_c; in this case, any conversion to differential-mode is not considered.

    To avoid the former problem, [10] and [11] transform the description of the two-port device from S-parameters to Z-parameters. Then, a floating current or voltage source is applied between the input ports of the device, instead of normalized power waves. These boundary conditions lead to a different input impedance definition which can be transformed back to S-parameters. Besides, an equivalent solution is found in [12] and [13] by means of applying the same floating signal sources to the two-port, but such boundary conditions are straightly expressed in terms of S-parameters, instead of transforming to Z-parameters. In both cases, the input impedance found shows the non-symmetrical response of the device. However, up to the author's knowledge no procedure expressing $\Gamma_d\left(\Gamma_c\right)$ or $Z_d\left(Z_c\right)$ in terms of S_{mm} has been yet proposed. Even more, all previous cases must be understood as particular cases of a general expression based on the definitions of mixed-mode scattering parameters and loads.

    Within this framework, the rest of this paper is devoted to extend the theory of mixed-mode scattering parameters not only to

symmetrical devices, but to non-symmetrical or actual devices. For this reason, in Section 2, a general expression of $\Gamma_d\left(\Gamma_c\right)$ will be obtained which resembles the well-known expressions of $\Gamma_{\text{in}}\left(\Gamma_{\text{out}}\right)$ for a single-ended two-port device. Such definitions will allow to obtain $Z_d\left(Z_c\right)$ in terms of S_{mm}. In Section 3, it is shown that former particular cases of the driving of a two-port device are reduced to the application of a short, open and matched mixed-mode load conditions on the general expression of $\Gamma_d\left(\Gamma_c\right)$. As a practical case in Section 4, an adequate definition of Q will be obtained, by means of Z_d, that allows the direct comparison between symmetrical and non-symmetrical inductors. Finally, the conclusions of this work are presented in Section 5.

2. INPUT REFLECTION COEFFICIENT OF A TWO-PORT DEVICE

When attempting to calculate $\Gamma_d\left(\Gamma_c\right)$, it is useful to keep in mind the definition of the input(output) reflection coefficient $\Gamma_{\text{in}}\left(\Gamma_{\text{out}}\right)$ of a two-port device. As it can be seen in Fig. 1, Γ_{in} is defined as the quotient between the incident power wave a_1 and the reflected power wave b_1 at the input port P_1, when a load Z_L has been connected to the output port. Besides, Γ_{out} is the reflection coefficient towards the output port P_2, when a source impedance Z_S has been connected to the input port [14, 15]. Due to the fact that there is a linear transformation between S and S_{mm}, i.e., $S = M^{-1}S_{mm}M$ [16], the two-port network in Fig. 1 can be represented as a two-port device where the input port and the output port have been substituted by a differential and common-mode ports. At this point, $\Gamma_d\left(\Gamma_c\right)$ can be correctly defined by analogy to $\Gamma_{\text{in}}\left(\Gamma_{\text{out}}\right)$. Consequently, $\Gamma_d\left(\Gamma_c\right)$ is the input reflection coefficient of a two-port device when exciting with a differential (common)-mode power wave meanwhile the two-port device is loaded with a common
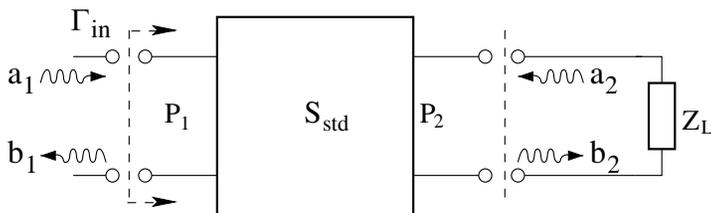
Figure 1. Input reflection coefficient of a two-port device in standard S-parameters.

(differential)-mode load.

2.1. Differential-mode Input Reflection Coefficient, Γ_d

Figure 2 shows how a differential power wave a_d is launched towards a two port device meanwhile a common-mode impedance Z_L^c is connected to the common-mode port. S_{mm} relates the incident and reflected differential and common-mode power waves by

$$\begin{pmatrix} b_d \\ b_c \end{pmatrix} = \begin{pmatrix} S_{dd} & S_{dc} \\ S_{cd} & S_{cc} \end{pmatrix} \begin{pmatrix} a_d \\ a_c \end{pmatrix}. \tag{3}$$

In this case, the two-port scatters back two power waves b_d and b_c. The common-mode reflected wave b_c reaches the common-mode load Z_L^c, which reflects a common-mode wave a_c. Thereby, it can be written the following relation

$$a_c = \Gamma_L^c b_c \tag{4}$$

where Γ_L^c is the reflection coefficient associated with Z_L^c. Replacing (4) in (3) and after some algebra, Γ_d is expressed as follows

$$\Gamma_d = \frac{S_{dd} - |S|\,\Gamma_L^c}{1 - S_{cc}\Gamma_L^c}. \tag{5}$$

Notice that, whenever a two-port is completely symmetric and balanced (i.e., $S_{11} = S_{22}$ and $S_{12} = S_{21}$, which lead to $S_{dc} = S_{cd} = 0$ and $|S| = S_{dd}S_{cc}$), Γ_d is equal to S_{dd} irrespective of the connected load Z_L^c. In this case, as it has been previously mentioned, Z_d matches Z_{dd}.

It is also interesting to rewrite (4) as a function of the incident power wave a_1 and a_2 at each port referred to the common ground. From [3], $a_{d(c)}$ and $b_{d(c)}$ read as

$$a_{d(c)} = \frac{1}{\sqrt{2}} \left(a_1 \mp a_2 \right)$$

$$b_{d(c)} = \frac{1}{\sqrt{2}} \left(b_1 \mp b_2 \right) \tag{6}$$
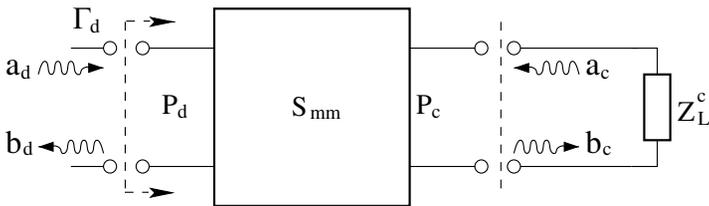
Figure 2. Differential-mode reflection coefficient of a two-port device in mixed-mode S-parameters.

where the upper and lower signs hold for the differential and common-mode, respectively. Substituting (6) in (4), the following relation is obtained

$$a_1 = -a_2 + \sqrt{2}\Gamma_L^c b_c. \tag{7}$$

Note that even though a differential power wave a_d is launched through the two-port device, a_1 equals $-a_2$ only in two cases: 1) $\Gamma_L^c = 0$, i.e., the common-mode load is a matched load; 2) $b_c = 0$, i.e., the two-port is purely balanced. For the remaining cases, a_1 differs from $-a_2$ due to the fact that a common-mode power wave a_c is scattered back by the common-mode load.

Keeping in mind the existing linear transformation between S and S_{mm} parameters, notice the duality of (5) when it is compared with the Γ_{in} (Γ_{out}) expression of the single-ended analysis of a two-port device

$$\begin{aligned}
\Gamma_{\text{in}} &= \frac{S_{11} - |S|\,\Gamma_L}{1 - S_{22}\Gamma_L} \\
\Gamma_{\text{out}} &= \frac{S_{22} - |S|\,\Gamma_S}{1 - S_{11}\Gamma_S}.
\end{aligned} \tag{8}$$

By means of this comparison, one realizes that, as in the single-ended case, three standard loads can be defined: a matched load ($\Gamma_L^c = 0$), an open-circuit ($\Gamma_L^c = 1$) and a short-circuit ($\Gamma_L^c = -1$). Notice that, each of these cases results in a different boundary condition when substituting $\Gamma_L^c = 0, 1, -1$ in (4) as it will be analyzed in Section 3.

2.2. Common-mode Input Reflection Coefficient, Γ_c

Whenever a common-mode power wave a_c is launched towards a two-port device, as it can be seen in Fig. 3, two power waves, b_d and b_c are scattered back. Now, b_d reaches the differential load, Z_L^d, which reflects a differential-mode normalized power wave a_d. The relationship established between a_d and b_d through Z_L^d is
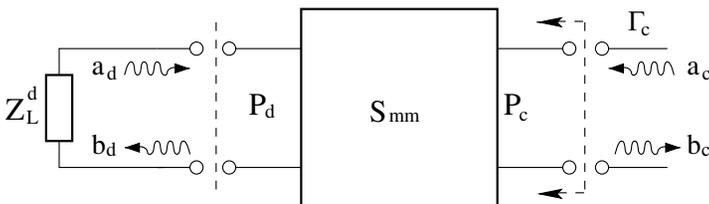
Figure 3. Common-mode reflection coefficient of a two-port device in mixed-mode S-parameters.

$$a_d = \Gamma_L^d b_d \qquad (9)$$

wherein Γ_L^d is the reflection coefficient of the differential-mode load. A dual expression of (5) can be written when substituting (9) in (3),

$$\Gamma_c = \frac{S_{cc} - |S|\,\Gamma_L^d}{1 - S_{dd}\Gamma_L^d}. \qquad (10)$$

Notice that, when the two-port is symmetric and balanced (i.e., $S_{dc} = S_{cd} = 0$ and $|S| = S_{dd}S_{cc}$), Γ_c equals S_{cc} irrespective of the connected load. As it has been previously mentioned, only in this case Z_c matches Z_{cc}.

By replacing (6) in (9), a_1 relates to a_2 as follows

$$a_1 = a_2 + \sqrt{2}\Gamma_L^d b_d. \qquad (11)$$

Therefore, even when a common-mode power wave a_c is launched through the two-port device, a_1 equals a_2 only in two cases: 1) $\Gamma_L^d = 0$, i.e., the differential-mode load is a matched load; or 2) $b_d = 0$, i.e., the two port is ideally balanced. Otherwise, a_1 differs from a_2. This is due to the fact that a differential-mode power wave a_d is reflected back by the differential-mode load.

Equation (10) represents the dual case of (5). Therefore, three differential mixed-mode load conditions can be defined by means of $\Gamma_L^d = 0,\ 1,\ -1$.

3. MIXED-MODE DRIVING CONDITIONS

Three driving conditions can be defined which lead to different boundary conditions for a two-port device and different expressions of $\Gamma_d\,(\Gamma_c)$. In order to explore these driving conditions, it is very illustrative to think about the theoretical realization of a true mixed-mode VNA as the one in Fig. 4. Notice that, in contrast to the two-port device in Fig. 3, the device represented in Fig. 4 is a physical realization where the two input ports and the existing common-ground can be associated to either a single-ended or a mixed-mode representation. Actually, the physical realization of a pure-mode VNA (PMVNA) is rather difficult and, even though some works have been conduced toward its consecution [17, 18], current multi-port VNAs implement Bockelman's formulation to display S_{mm}. In fact, a commercial PMVNA is not yet available.

It is also important to notice that the DUT is normally connected to the PMVNA by means of a pair of coupled transmission lines and a ground reference which allows the propagation of differential and common-mode power waves. However, as it has been previously
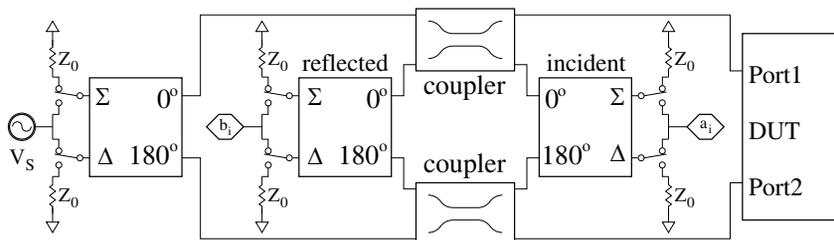
Figure 4. Pure-mode vector network analyzer.

demonstrated in [3], if the even and odd-mode characteristic impedance are chosen to be equal, such reference coupled lines can be considered uncoupled transmission lines. Even more, as it is also mention, there is not restriction for the length of the reference lines, thus zero length transmission lines can be defined and (6) still holds on.

3.1. Matched Load $\Gamma_L^{d(c)}=0$

Whenever a power wave is launched from the V_s generator in Fig. 4, a switchable $0°/180°$ hybrid generates either a differential a_d or common-mode a_c power waves. These incident waves can be measured by setting accordingly the $0°/180°$ input at the incident wave hybrid. When the selected power wave reaches the DUT, the incident power wave is scattered back, as well as an opposite mode wave is generated due to the asymmetry of the two-port device. Both modes can be measured by setting the switchable $0°/180°$ reflected wave hybrid. It is important to notice that whenever one mode is selected, the opposite mode is connected to its surge impedance $2Z_0$ or $Z_0/2$ through each hybrid, thus non scattered wave from the loads is allowed. This assumption is similar to connect Z_0 at the opposite port with respect to the one that is being measured when the measure of S_{11} or S_{22} is done by means of a classical VNA. Assuming the condition that the incoming wave is a_d, and keeping in mind that $\Gamma_L^c = 0$, from (5) Γ_d reads as

$$\Gamma_d = S_{dd}. \qquad (12)$$

In this case, from (4) a_c is equal to zero. Thus, a_1 equals $-a_2$. Only when the reflected power wave is absorbed in the common-mode load, the normalized power waves ingoing into the two-port device are equal in magnitude and opposite sign, thus they are pure differential signals. Besides, whenever it is assumed that $a_1 = -a_2$, this condition always leads to $\Gamma_d = S_{dd}$, even though a_c differs actually from zero in an actual measurement setup. Then, it is not surprising that, when attempting to calculate Γ_d by means of a $0°/180°$ hybrid or an equivalent device

terms of mixed-mode S-parameters. Proceeding in this way, both S_{mm} and circuit theory are shown to be mathematically equivalent and, additionally, the goodness of the bilineal impedance transformation is highlighted.

Thus, when $\Gamma_L^c = 1$, (7) can be rewritten as

$$a_1 = -a_2 + \sqrt{2}b_c. \tag{17}$$

As it has been previously mentioned, a_1 differs from a_2 except when the two port is purely symmetric. Otherwise, replacing b_c by (6) and by means of the following expressions [3]

$$
\begin{aligned}
V_i &= \sqrt{Z_0}\,(a_i + b_i) \\
I_i &= \frac{1}{\sqrt{Z_0}}\,(a_i - b_i)\,,
\end{aligned}
\tag{18}
$$

(17) can be written as $I_1 = -I_2$. It means that the normalized power waves can be replaced by a floating current source as it is shown in Fig. 5 and the result is equivalent to (15). Consistently, the condition $I_1 = -I_2$ implies that there is no common-mode current flowing into the device; thus, from the point of view of the common-mode, it can be seen as an open load, i.e., $\Gamma_L^c = 1$.

In order to calculate Z_d, both currents can be expressed in terms of S-parameters as follows

$$
\begin{aligned}
I_1 &= \frac{1}{\sqrt{Z_0}}\,(a_1 - b_1) = \frac{1}{\sqrt{Z_0}}\,[(1 - S_{11})\,a_1 - S_{12}a_2] \\
I_2 &= \frac{1}{\sqrt{Z_0}}\,(a_2 - b_2) = \frac{1}{\sqrt{Z_0}}\,[-S_{21}a_1 + (1 - S_{22})\,a_2]\,.
\end{aligned}
\tag{19}
$$

Thus, a_2 can be written in terms of a_1:

$$a_2 = -\frac{a_1\,(-1 + S_{11} + S_{21})}{-1 + S_{22} + S_{12}} = -a_1\frac{S_{cc} + S_{cd} - 1}{S_{cc} - S_{cd} - 1}. \tag{20}$$

Note that for a symmetric and reciprocal two-port device (i.e., $S_{dc} = S_{cd} = 0$), (20) results in $a_2 = -a_1$. Otherwise, the ingoing waves are different at each port, and such difference depends on S_{cc} and S_{cd} which convey a common-mode conversion. Now, by means of (20), the voltage and currents at each node of the DUT can be rewritten as a function of a_1 as

$$V_i = \sqrt{Z_0}\,a_1\left\{\pm\frac{S_{dd} - S_{cc} + 1 - |S|}{1 - S_{cc} + S_{cd}} + \frac{2S_{cd}}{1 - S_{cc} + S_{cd}}\right\} \tag{21}$$

$$I_1 = -I_2 = \frac{1}{\sqrt{Z_0}}\,a_1\frac{S_{dd} - S_{cc} - 2S_{cd} + 1 - |S|}{1 - S_{cc} + S_{cd}} \tag{22}$$

where in (21) the upper and lower signs hold for port 1 and port 2, respectively. As a matter of fact, only when the two-port device is symmetric, (21) results in $V_1 = -V_2$.

From (21) and (22), $V_d = V_1 - V_2$ and $I_d = I_1 = -I_2$ can be calculated and, since Z_d is V_d/I_d, it reads as follows

$$Z_d = Z_0 \left(\frac{1 + S_{dd} + S_{dc}}{1 - S_{dd} - S_{cd}} + \frac{(1 + S_{dd} - S_{dc})(1 - S_{cc} - S_{cd})}{(1 - S_{dd} - S_{cd})(1 - S_{cc} + S_{cd})} \right). \quad (23)$$

Likewise Γ_d, in some cases, (23) can lead to an indetermination if it is directly developed. In order to avoid such indetermination, Z_d can be naturally split into two cases: 1) the two-port is ideally symmetric, which means that the second term in (23) can be simplified since $S_{cd} = S_{dc} = 0$; 2) otherwise (even when designing the device as a differential component). Therefore, Z_d is expressed as follows

$$Z_d = \begin{cases} 2Z_0 \dfrac{1 + S_{dd}}{1 - S_{dd}} & \text{if } S_{dc} = S_{cd} = 0 \\ 2Z_0 \dfrac{S_{dd} - S_{cc} + 1 - |S|}{1 + |S| - S_{dd} - S_{cc}} & \text{Otherwise} \end{cases}. \quad (24)$$

As it was expected, Z_d matches Z_{dd} only when the two-port is symmetric. It can be seen that, the same result is obtained by applying the bilineal transformation (16) to (15). Therefore, the former theory is consistent with circuit theory.

3.3. Γ_c when $\Gamma_L^d = 1$

Replacing $\Gamma_L^d = 1$ in (10), Γ_c results as follows

$$\Gamma_c = \frac{S_{cc} - |S|}{1 - S_{dd}}. \quad (25)$$

Also in this case, when the device is purely balanced and floating (i.e., $S_{dd} = 1$ and $|S| = S_{cc}$), (25) results in an indetermination. This indetermination is naturally solved by using (10) and Γ_c results in S_{cc}. If the device is simply symmetric and non-mode conversion is allowed, (i.e., $S_{dc} = S_{cd} = 0$), Γ_c results in S_{cc}.

Moreover, when $\Gamma_L^d = 1$ and (18) are inserted in (11), it is obtained that $I_1 = I_2$. Then, the normalized power waves can be replaced by two equivalent current sources connected at both ports as it is shown in Fig. 5. This equivalent driving condition is also consistent if one realizes that no differential current is allowed, thus from the point of view of the differential-mode, this boundary condition is seen as an open circuit.

In order to calculate Z_c, (25) is substituted in the following bilineal transformation

$$Z_c = \frac{Z_0}{2}\frac{1+\Gamma_c}{1-\Gamma_c}. \tag{26}$$

Therefore the common-mode impedance Z_c when $\Gamma_L^d = 1$ results

$$Z_c = \begin{cases} \dfrac{Z_0}{2}\dfrac{1+S_{cc}}{1-S_{cc}} & \text{if } S_{dc}=S_{cd}=0 \\[2mm] \dfrac{Z_0}{2}\dfrac{S_{dd}-S_{cc}-1+|S|}{S_{dd}+S_{cc}-1-|S|} & \text{Otherwise} \end{cases}. \tag{27}$$

As expected, only in the case when the two-port is symmetric Z_c matches with Z_{cc}.

3.4. Γ_d when $\Gamma_L^c = -1$

When $\Gamma_L^c = -1$, Γ_d is given by
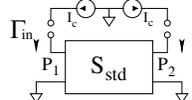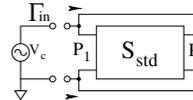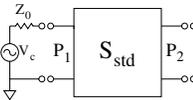
$$\Gamma_d = \frac{S_{dd}+|S|}{1+S_{cc}}. \tag{28}$$

Again, if the device is purely symmetric (i.e., $S_{dc} = S_{cd} = 0$ and $|S| = S_{dd}S_{cc}$), Γ_d results in S_{dd} as expected. It is also interesting to write (7) when $\Gamma_L^c = -1$,

$$a_1 = -a_2 - \sqrt{2}b_c. \tag{29}$$

As it has been previously mentioned, a_1 differs from $-a_2$ except when the two port is purely symmetric. Otherwise, replacing b_c by (6) and by means of (18), $V_1 = -V_2$. Again, the power waves sources can be replaced by single-ended voltage sources as it is shown in Fig. 5. Notice from Fig. 5 that the common-mode node between the differential voltage sources is shorted, thus $\Gamma_L^c = -1$.

Thus, Z_d can be calculated replacing (28) in the impedance

Γ_L^d	1	1	0
b.c.	$I_1 = I_2$	$V_1 = V_2$	$a_1 = a_2$
Γ_c Equivalent driving method			
Expression	$\dfrac{S_{cc} - |S|}{1 - S_{dd}}$	$\dfrac{S_{cc} + |S|}{1 + S_{dd}}$	S_{cc}

Figure 5. Two-port mixed-mode driving topologies.

transformation (16),

$$Z_d = \begin{cases} 2Z_0 \dfrac{1 + S_{dd}}{1 - S_{dd}} & \text{if } S_{dc} = S_{cd} = 0 \\[2mm] 2Z_0 \dfrac{S_{dd} + S_{cc} + 1 + |S|}{1 - |S| - S_{dd} + S_{cc}} & \text{Otherwise} \end{cases} . \tag{30}$$

3.5. Γ_c when $\Gamma_L^d = -1$

Replacing $\Gamma_L^d = -1$ in (10), Γ_c reads as

$$\Gamma_c = \frac{S_{cc} + |S|}{1 + S_{dd}}. \tag{31}$$

Likewise in the previous cases, when the device is symmetric (i.e., $S_{dc} = S_{dc} = 0$ and $|S| = S_{dd}S_{cc}$), Γ_c results in S_{cc}. Once more, rewriting (11) when $\Gamma_L^d = -1$,

$$a_1 = a_2 - \sqrt{2}b_d. \tag{32}$$

As it has been previously mentioned, a_1 differs from a_2 except when the two port is purely symmetric. Otherwise, replacing b_d by (6) and by means of (18), $V_1 = V_2$. In this case, the power waves can be replaced by a voltage source connected to both ports as in Fig. 5. Therefore, any differential voltage source has been shorted; it implies that from the point of view of the differential-mode, Γ_L^d equals -1.

A new expression for Z_c can be calculated replacing (31) in (26),

$$Z_c = \begin{cases} \dfrac{Z_0}{2} \dfrac{1 + S_{cc}}{1 - S_{cc}} & \text{if } S_{dc} = S_{cd} = 0 \\[2mm] \dfrac{Z_0}{2} \dfrac{S_{dd} + S_{cc} + 1 + |S|}{1 - |S| + S_{dd} - S_{cc}} & \text{Otherwise} \end{cases} . \tag{33}$$

At this point, a set of different expressions for $\Gamma_d (\Gamma_c)$ and $Z_d (Z_c)$ have been obtained through driving a two-port device with

different standard mixed-mode loads. As it has been previously shown, these expressions can be applied to non-symmetrical two-port devices. However, it is important to notice that each of these expressions are only valid for a specific boundary conditions which are summarized in Fig. 5.

4. PRACTICAL CASE

An integrated inductor can be considered as a two-port device similar to the one on Fig. 2. Thus, the former theory can be applied to the evaluation of the quality factor, Q, of inductors. Q is defined as a ratio of the stored reactive energy over the energy loss evaluated in one cycle. However, this definition is quite subtle because the stored energy is actually dependent on the shape of electromagnetic fields around the component. These fields are related to the geometry, including layout elements nearby; but, most important, to the way in which the inductor is excited in [21–23]. Noticing the benefit of exciting inductors differentially, Rabjohn introduced the use of symmetrical shapes in the implementation of fully differential RFICs substituting traditional spiral ones [24, 25]. Thus, for any inductor, Q is given by

$$Q = \frac{\text{Im}\{Z_d\}}{\text{Re}\{Z_d\}}, \tag{34}$$

where, as demonstrated previously, for an ideal symmetric inductor Z_d results in Z_{dd}. However, even though a symmetrical shape is used in their implementation, symmetry is not always guaranteed. Indeed, cross-bridges sections or layout asymmetries at the surrounding area of an inductor can break the symmetry of its own electromagnetic fields. Furthermore, there is still many situations in which spiral inductors can be preferred over symmetrical ones, e.g., when one of the terminal of the inductor is grounded, or when area reduction prevails over symmetry [26, 27]. For these cases, the choice between symmetric and spiral topologies is currently set through the comparison of the Q factor when driving the device differentially. Thereby, it is important to find the correct definition of Q for both topologies, i.e., it must be avoided that any inductor shape benefits itself from the definition of the Q factor. To proceed with, the previously developed theory and concepts provide a correct framework for such comparison.

Figure 6 shows two inductors using different topologies, symmetric and spiral, that have been synthesized using layout optimization techniques [28] for a given application in the frequency range of 2.45 GHz using a 0.35 μm CMOS technology. Their geometrical characteristics are summarized in Table 1. Notice that both geometries
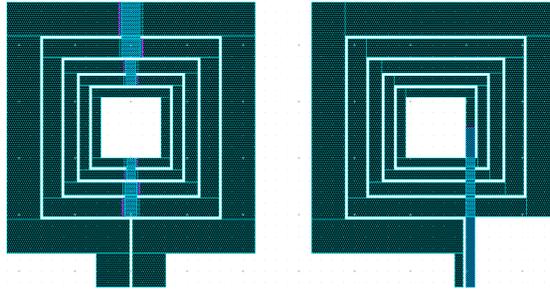
**Figure 6.** Symmetric and spiral optimazed inductors layout.

Table 1. Geometrical characteristics of both inductors.

|	
Number of turns	5
Inner diameter [μm]	54
Spacing between turns [μm]	2.5
Width of the first turn (inner turn) [μm]	7.8
Width of the second turn [μm]	8.6
Width of the third turn [μm]	11.1
Width of the fourth turn [μm]	16.8
Width of the fifth turn (outer turn) [μm]	30

are quite similar, thus a similar Q factor behavior should be expected. Both layouts have been simulated with MoMemtum, a planar solver from Agilent Technologies, obtaining the two-port single-ended S-parameter matrix over a frequency range beyond the Self Resonance Frequency (SRF). The obtained S-parameters are later mathematically converted to mixed-mode S-parameters matrix description [6].

When exciting symmetric inductors differentially, non reflected common-mode power wave exist which means that the response of the component is independent of the common-mode load Γ_L^c, as it has been previously demonstrated. Then, Z_d equals Z_{dd} and (2) and (34) are equivalent. Fig. 7 shows a plot of the Q factor value for the previous given symmetrical inductor when loaded with $\Gamma_L^c = 0$, 1 and -1. As expected, all the cases give the same Q factor behavior.

On the contrary, the differential excitation of a spiral inductor allows the existence of a common-mode reflected power wave. Therefore, the response of the device is dependent on the value of the common-mode load Γ_L^c. Using the same common-mode load conditions as in the previous symmetrical case (i.e., open, short and match), Fig. 8 shows the behavior of Q for the non-symmetric inductor. It is worth
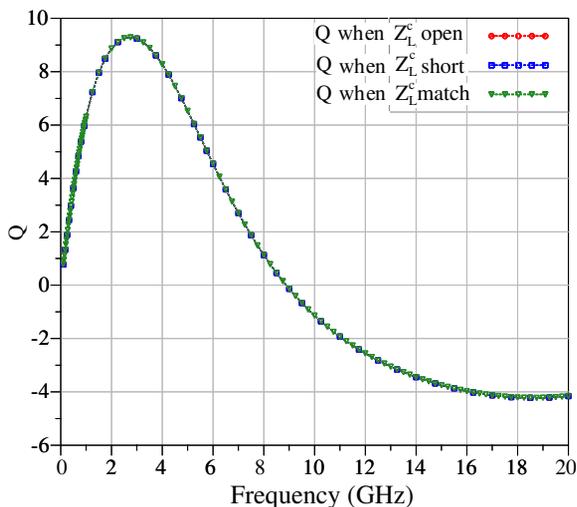
Figure 7. Quality factor vs. frequency for a symmetric inductor using (34) when $Z_L^c = Z_0/2$ (match), open, short.
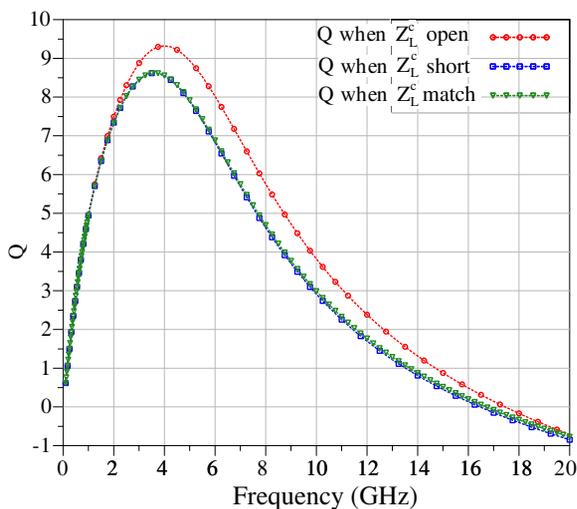
Figure 8. Quality factor vs. frequency for an asymmetric inductor using (34) when $Z_L^c = Z_0/2$ (match), open, short.

noting that differences larger than a 10% can be obtained depending on the boundary condition, i.e., the value of Q can be boosted just because of the definition of Q itself. Therefore, once an inductor is chosen, the main issue is to identify the correct boundary conditions which lead to the adequate value of Q.

5. CONCLUSIONS

The theory of mixed-mode scattering parameters has been extended not only to symmetrical devices, but to non-symmetrical or actual devices, finding a general expression for $\Gamma_d\left(\Gamma_c\right)$ that resembles the well-known expressions of $\Gamma_{\text{in}}\left(\Gamma_{\text{out}}\right)$ for a single-ended two-port device. It has also been shown that the former particular cases of the driving of a two-port device are reduced to the application of a short, open and matched mixed-mode load conditions on the general expression of $\Gamma_d\left(\Gamma_c\right)$. Moreover, such definitions allow to obtain $Z_d\left(Z_c\right)$ in terms of S_{mm}. An analytic connection between scattering-parameters description in both versions, through the use of S-parameters and S_{mm}, and lumped elements description has naturally been used toward the consecution of these expressions. As a practical case, the Q value for symmetrical and non-symmetrical inductors has been obtained using the definition of Z_d, illustrating the differences when considering different boundary conditions.

ACKNOWLEDGMENT

REFERENCES

1. Amin, Y. and H. Tenhunen, "Development and analysis of exible UHF RFID antennas for "green" electronics," *Progress In Electromagnetics Research*, Vol. 130, 1–15, 2012.

2. Wu, S.-M., C.-T. Kuo, P.-Y. Lyu, Y. L. Shen, and C.-I. Chien, "Miniaturization design of full differential bandpass filter with coupled resonators using embedded passive device technology," *Progress In Electromagnetics Research*, Vol. 121, 365–379, 2011.

3. Bockelman, D. E. and W. R. Eisenstadt, "Combined differential and common-mode scattering parameters: Theory and simulation," *IEEE Transactions on Microwave Theory and Techniques*, Vol. 43, No. 7, 1530–1539, Jul. 1995.

4. Bockelman, D. E. and W. R. Eisenstadt, "Combined differential and common-mode analysis of power splitters and combiners," *IEEE Transactions on Microwave Theory and Techniques*, Vol. 43, No. 11, 2627–2632, Nov. 1995.

5. Skyworks Application Note, "Matching differential port device," Skyworks Solutions, Inc., Oct. 2009.

6. Danesh, M., "Monolithic inductors for silicon radio frequency integrated circuits," M. A. Sc. Thesis, Dept. Elect. Comput. Eng., Univ. Toronto, Toronto, ON, Canada, 1999.

7. Danesh, M. and J. R. Long, "Differentially driven symmetric microstrip inductors," *IEEE Transactions on Microwave Theory and Techniques*, Vol. 50, No. 1, 332–341, Jan. 2002.

8. Kuo, S. K., S. L. Chen, and C. T. Lin, "An accurate method for impedance measurement of RFID tag antenna," *Progress In Electromagnetics Research*, Vol. 83, 93–106, 2008.

9. Danesh, M. and J. R. Long, "Authors' reply," *IEEE Transactions on Microwave Theory and Techniques*, Vol. 55, No. 4, 809–810, Apr. 2007.

10. Meys, R. and F. Janssens, "Measuring the impedance of balanced antennas by an S-parameter method," *IEEE Antennas and Propagation Magazine*, Vol. 40, No. 6, 62–65, Dec. 1998.

11. Qing, X. and Z. N. Chen, "Impedance characterization of RFID tag antennas and application in tag co-design," *IEEE Transactions on Microwave Theory and Techniques*, Vol. 57, No. 5, 1268–1274, May 2009.

12. Konstroffer, L., "Finding the reflection coefficient of a differential one-port device," *RF Semiconductor*, 1999.

13. Drakaki, M., A. A. Hatzopoulos, and A. Siskos, "CMOS inductor performance estimation using Z- and S-parameters," *IEEE International Symposium on Circuits and Systems, ISCAS*, 2256–2259, 2007.

14. Collin, R. E., *Foundations for Microwave Engineering*, 2nd Edition, Wiley-IEEE Press, Dec. 2000.

15. Liang, C. H., Y. Shi, and T. Su, "S parameters theory of lossless block network," *Progress In Electromagnetics Research*, Vol. 104, 253–266, 2010.

16. Wloczysiak, S., "Match the ports of differential devices," *Microwaves and RF*, ED Online ID #22407 Edition, Feb. 2010.

17. Bockelman, D. E. and W. R. Eisenstadt, "Pure-mode network analyzer for on-wafer measurements of mixed-mode S-parameters of differential circuits," *IEEE Transactions on Microwave Theory*

and Techniques, Vol. 45, No. 7, 1071–1077, Jul. 1997.

18. Zwick, T. and U. R. Pfeiffer, "Pure-mode network analyzer concept for on-wafer measurements of differential circuits at millimeter-wave frequencies," *IEEE Transactions on Microwave Theory and Techniques*, Vol. 53, No. 3, 934–937, Mar. 2005.

19. Qing, X. and Z. N. Chen, "Comments on 'measuring the impedance of balanced antennas by an S-parameter method'," *IEEE Antennas and Propagation Magazine*, Vol. 52, No. 1, 171–172, Feb. 2010.

20. Kaldjob, E., B. Geck, and H. Eul, "Comments on 'measuring the impedance of balanced antennas by an S-parameter method'," *IEEE Antennas and Propagation Magazine*, Vol. 50, No. 6, 113–114, Dec. 2008.

21. Pan, S. J., L. W. Li, and W. Y. Yin, "Performance trends of on-chip spiral inductors for RFICs," *Progress In Electromagnetics Research*, Vol. 45, 123–151, 2004.

22. Carrillo, T. C., J. G. Macias-Montero, A. O. Marti, J. S. Cordoba, and J. M. Lopez-Villegas, "CMOS single-ended-to-differential low-noise amplifier," *Integration, the VLSI Journal*, Vol. 42, No. 3, 304–311, 2009, Special Section on DCIS2006.

23. Aluigi, L., F. Alimenti, and L. Roselli, "Automatic design and 3D electromagnetic simulation of sub-nH spiral inductors," *PIERS Proceedings*, 1719–1722, Marrakesh, Morocco, Mar. 20–23, 2011.

24. Rabjohn, G. G., "Monolithic microwave transformers," M. Eng. Thesis, Carleton University, Ottawa, ON, Canada, Apr. 1991.

25. Zheng, Y. and C. E. Saavedra, "Frequency response comparison of two common active inductors," *Progress In Electromagnetics Research Letters*, Vol. 13, 113–119, 2010.

26. Abdullah, E., "Planar inductor design for high power applications," *Progress In Electromagnetics Research B*, Vol. 35, 53–67, 2011.

27. Wang, R., J. Xu, C.-L. Wei, M.-Y. Wang, and X.-C. Zhang, "Improved extraction of coupling matrix and unloaded Q from S-parameters of lossy resonator filters," *Progress In Electromagnetics Research*, Vol. 120, 67–81, 2011.

28. Lopez-Villegas, J. M., J. Samitier, C. Cane, P. Losantos, and J. Bausells, "Improvement of the quality factor of RF integrated inductors by layout optimization," *IEEE Transactions on Microwave Theory and Techniques*, Vol. 48, No. 1, 76–83, Jan. 2000.